J Mater Sci (2010) 45:1117–1122
DOI 10.1007/s10853-009-4054-y

Direct synthesis and characterization of LaSBA-15 mesoporous molecular sieves

Geraldo E. Luz Jr. · Stevie H. Lima · Ana C. R. Melo · Antonio S. Araujo · Valter J. Fernandes Jr.

Received: 7 September 2009 / Accepted: 19 November 2009 / Published online: 1 December 2009

Abstract Lanthanum-incorporated SBA-15 mesoporous molecular sieves were synthesized in a two-stage hydrothermal procedure from a precursor solution containing lanthanum chloride. The products were characterized by powder X-ray diffraction, thermogravimetric analysis, X-ray fluorescence, and nitrogen porosimetry. Taken together, the analyses indicated that the products formed highly ordered mesostructures with large average pore sizes, and suggested that the lanthanum was incorporated in the SBA-15 both into the framework as well as within the mesopores. Catalytic dehydration of ethanol over the LaSBA-15 products shows that they have weak Lewis acid and basic functionalities, indicative of the presence of lanthanum oxide in these samples.

Introduction

The mesoporous molecular sieves represent a class of inorganic materials that have a high surface area and accessible pores to relatively large molecules. For that, it is recognized as a class of materials with a great potential for absorption and catalysis. Among this class, the SBA-15 is regarded as one of the most promising materials due to its high hydrothermal and thermal stability, besides its high surface area and large pore size [1, 2]. On the other hand, the pure silica SBA-15 shows low-catalytic activity due to the absence of heteroatom activity sites [3–5]. Therefore, it is of great importance to introduce a heteroatom into the mesopores these molecular sieves, especially metals. Among these metals, cerium and lanthanum have widely been used in the catalysts, and show a significant improvement of the hydrothermal and thermal stability of the molecular sieves, and an increase of the acidity of these materials [3, 6–13]. However, the incorporation of a metal into the SBA-15 is not an easy task. The high solubility of the metal ion in the strong acidic environment, in which the hydrothermal synthesis of SBA-15 is usually performed, hinders the metal incorporation. Given that fact, recent studies [8, 9, 13–20] have reported the pH-adjusting of the synthesis gel at values higher than 2 as a way to facilitate the metal incorporation into SBA-15. Based on these works, La-incorporated SBA-15 mesoporous molecular sieves were directly synthesized by pH-adjusting of the synthesis gel at 6 with *n*-butyl amine. The synthesized materials were characterized by power X-ray diffraction (XRD), X-ray fluorescence (XRF), thermal analysis, and nitrogen sorption. The active sites of the samples were characterized by the ethanol dehydration reaction.

Experimental

Synthesis

Lanthanum-incorporated SBA-15 mesopores molecular sieves (LaSBA-15) were synthesized as follows: 4.0 g of Pluronic P123, used as a template, was dissolved in 148.3 mL of aqueous HCl solution of pH < 0.1 under stirring for 3 h at a temperature of 313 K. Thereafter, 8.8 mL of tetraethyl orthosilicate and a determined amount of hydrated lanthanum chloride (Si/La = 25, 50, and 75) were added, and the resulting mixture was stirred for 24 h

G. E. Luz Jr. (✉) · S. H. Lima · A. C. R. Melo · A. S. Araujo · V. J. Fernandes Jr.
Laboratory of Catalysis and Petrochemical, Department of Chemistry, Nature Science Center, Federal University of Rio Grande do Norte, Natal, RN 59078-970, USA
e-mail: geraldoeduardo@gmail.com

at a temperature of 313 K. The resulting gel was placed into a Teflon container and submitted to hydrothermal treatment at a temperature of 373 K for 24 h. After that, the reactive hydrogel was cooled down to room temperature, and its pH was adjusted at 6 with anhydrous *n*-butyl amine. Then, the gel was again submitted to hydrothermal treatment at the same temperature aforementioned, for more 24 h. After this time, the solid obtained was filtered, washed with anhydrous ethanol, dried at room temperature for 48 h, and finally calcined using a two-step procedure. In the first step of calcination, the solid was heated at 723 K, under flowing nitrogen (100 mL/min) for 2 h, and next heated at the same temperature under flowing dry air (100 mL/min) for additional 2 h. The calcination temperature reached a heating rate of 10 K/min. The samples prepared by this procedure were designated as La_xSBA-15, where *x* refers to molar ration Si/La.

Pure silica SBA-15 was prepared by similar procedure to the synthesis of LaSBA-15, but without the addition of hydrated lanthanum chloride, and was designated as SiSBA-15.

Characterization

The power XRD patterns of the calcined samples were recorded on a Shimadzu XRD 6000 power diffractometer using Ni filter, Cu Kα radiation (30 kV and 30 mA). The diffractograms were recorded in the 2θ range of 0.5°–5°. The molar ration Si/La in the calcined samples was determined by XRF on an EDX-700 of the Shimadzu. The thermal analysis for uncalcined samples were carried out on a Mettler Toledo 851 thermogravimetric analyzer under flow of helium (25 mL min^{-1}) from room temperature up to 1,173 K with a heating rate of 10 K/min. The nitrogen adsorption and desorption isotherms were measured at a temperature of 77 K on an ASAP-2010 model volumetric adsorption analyzer (Micromeritics). Prior to adsorption measurements each sample was degassed at temperature of 573 K for 2 h. The specific surface area was determined by the BET method and the total pore volume by the single point method. The BJH method was used to estimate the average pore size and the *t*-plot method was employed to assess the microporosity of the samples and estimate the volume and surface area of the micropores.

Ethanol dehydration

The ethanol dehydration reaction was carried out in a fixed-bed down-flow reactor. The samples (60 mg) were pre-treated at 773 K for 2 h in a flow of H_2 gas. Ethanol was fed into the catalyst bed at 773 K using H_2 (37 mL min^{-1}) as the carrier gas. The products were injected on line in a gas chromatograph Varian CP3800 equipped with detector of thermal conductivity and a dimethylpolysiloxane column (60 m, 0.53 mm, 5 μm) at intervals of 15 min. The products were identified by comparison of retention times of peaks in each chromatogram with retention times of standards of ethanol, water, diethyl ether, acetaldehyde, natural gas, and ethylene. Then, the ethanol conversion, the ethylene selectivity, and acetaldehyde selectivity were calculated.

Results and discussion

La-content by XRF

In Table 1 are shown the La-content in the solid LaSBA-15 samples. As expected the La-content in solid samples is lower than in the gel. However, when compared to the results of similar recent works [8, 9, 13, 16], the amount of lanthanum incorporated into the SBA-15 is relatively high. Moreover, it was noted that the percentage of lanthanum incorporated has increased with the declining of the ratio Si/La in the synthesis gel, reaching the highest value (56.3%) in the La_{25}SBA-15 sample. These results can be explained by the pH-adjusting of the synthesis gel at 6, after 24 h of hydrothermal treatment. The increase of the concentration of OH^-groups causes an increase in the concentration of the $[La(OH)_n]^{(3-n)}$ species, which are less soluble than the metal ion alone and, therefore, can facilitate the incorporation of the lanthanum into the SBA-15.

XRD

The XRD patterns of SiSBA-15 and LaSBA-15 samples are shown in Fig. 1. All the samples display three well-resolved diffraction peaks indexed as the (100), (110), and (200) diffractions. They reflect the two-dimensional hexagonal mesostructure with a space group of P6mm symmetry [1, 2], indicating that the pH-adjusting of the synthesis gel, after 24 h of hydrothermal treatment, and the La-incorporation into the SBA-15 has not destroyed the characteristic structure of the molecular sieve. It has also been observed that the intensity of these peaks has grown with the lanthanum incorporation, which indicates that the crystallographic properties of the SBA-15 have increased

Table 1 La-content in the LaSBA-15 samples

Samples	Si/La in the gel	Si/La in the solid	La incorporated[a] (%)
La_{75}SBA-15	75	319.6	24.4
La_{50}SBA-15	50	143.9	34.5
La_{25}SBA-15	25	44.6	56.3

[a] In relation to La-content in the synthesis gel

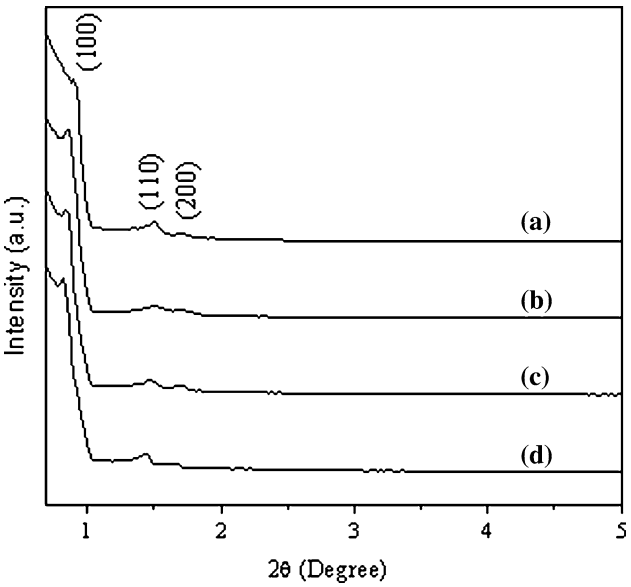

Fig. 1 XRD patterns of SiSBA-15 (*a*), La_{75}SBA-15 (*b*), La_{50}SBA-15 (*c*), and La_{25}SBA-15 (*d*)

with the metal incorporation. Furthermore, the 2θ values of the peak (100) have shifted toward lower values with the increasing of the La concentration, indicating that the unit-cell (a_0) has increased with the metal incorporation. Similar observations were also reported by earlier works [8, 9, 13, 16–18] and may have been caused by the increase of the wall thickness or of the average pore size, which can indicate an incorporation into the framework of the molecular sieve by formation of La–O–Si bonds, since the La–O is longer than the Si–O bond and thus can raise the average pore size.

Thermal analysis

The TG and DTG curves for the uncalcined samples are shown in Fig. 2A, B, respectively. Except for the SiSBA-15, all the samples have presented three steps of mass loss correlated, respectively, to thermo desorption of physically adsorbed water, P123 decomposition and water from condensation of superficial $[Si(OH)_n]^{(4-n)}$ and $[La(OH)_n]^{(3-n)}$ groups [21]. The quantitative information of the thermal analysis is shown in Table 2. Comparing this information with the results shown in Table 1, it verifies that the value of the third mass loss of the LaSBA-15 samples decreased with the increasing of the La-content, being more intensive in the La_{75}SBA-15, which presents the lowest amount of La-incorporated. As this mass loss is associated to the water output from the condensation of superficial $[Si(OH)_n]^{(4-n)}$ and $[La(OH)_n]^{(3-n)}$ groups, this fact can indicate that lanthanum was incorporated in the form of metallic oxide on the molecular sieve surface. On the other hand, the non-increase of the third mass loss with the increasing of the La-content indicates that lanthanum was not incorporated exclusively of that form. Another fraction of the initial amount of lanthanum may have been incorporated into the SBA-15 structure by way of La–O–Si bonds, as it was already indicated by XRD results.

Table 2 Quantification of the mass losses of the uncalcined samples in the thermal analysis

Samples	Temperature range (K)			Mass loss (%)		
	I	II	III	I	II	III
SiSBA-15	298–379	379–610	–	10.1	39.6	–
La_{75}SBA-15	301–372	372–527	527–876	12.8	9.3	30.9
La_{50}SBA-15	301–372	372–532	532–876	22.9	16.2	25.2
La_{25}SBA-15	303–371	371–536	536–876	17.5	12.6	25.2

As mentioned before, the SiSBA-15 has not presented three steps of mass loss. The third mass loss was not observed in this sample. This fact, associated to higher intensity of second mass loss in relation to other samples, also shown in Fig. 2 and Table 2, can indicate that the pH-adjusting of the

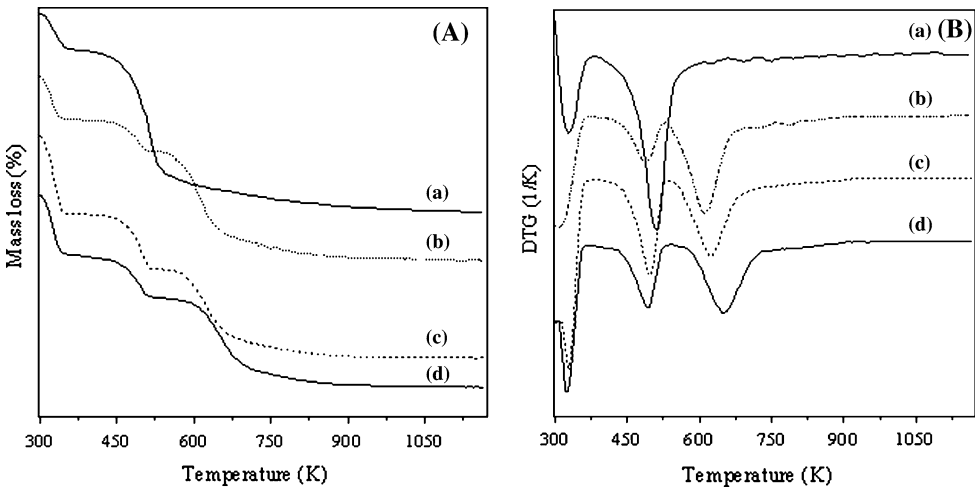

Fig. 2 TG (**A**) and DTG (**B**) curves of the uncalcined samples: SiSBA-15 (*a*), La_{75}SBA-15 (*b*), La_{50}SBA-15 (*c*), and La_{25}SBA-15 (*d*)

synthesis gel at 6 facilitated the $[Si(OH)_n]^{(4-n)}$ groups condensation, decreasing the temperature in which happens this condensation.

Nitrogen adsorption–desorption isotherms

The nitrogen adsorption–desorption isotherms of the samples are shown in Fig. 3. All the samples have the type-IV isotherm with a H1 hysteresis loop that is representative of mesopores materials [22, 23], and is in agreement with XRD results. The textural properties obtained from these isotherms and XRD patterns are shown in Table 3. The average pore size of LaSBA-15 samples is lower than the SiSBA-15 sample. Also, it has shifted toward higher values with the increasing of the La-content although it has not been a linear correlation. The first fact can indicate that a fraction of the lanthanum was incorporated into SBA-15 in the form of a metallic oxide thin layer within the mesopores, which may have caused the decrease in the average pore size. The second one, it indicates that the lanthanum also may have been incorporated into the framework of SBA-15, as this increase of pore size may be due to the La–O greater length in comparison to the Si–O bond [7, 8, 11, 13, 17]. Moreover, this fact can indicate that the incorporation into the framework becomes predominant with the increase of La concentration in the synthesis gel.

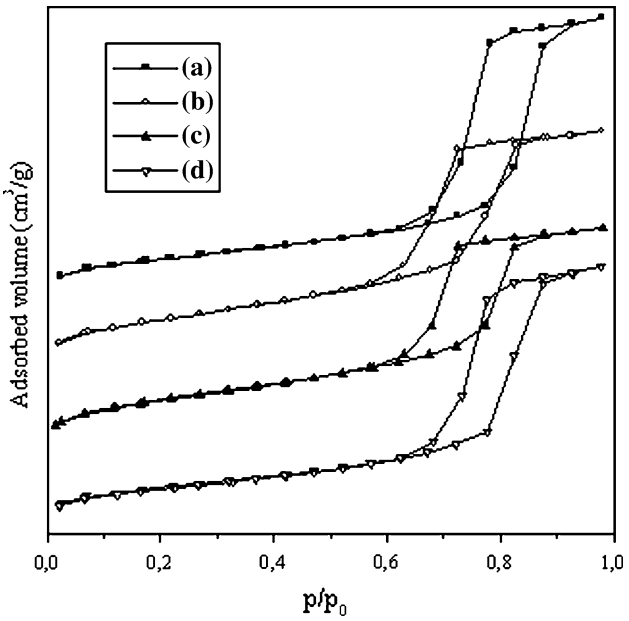

Fig. 3 Nitrogen adsorption–desorption isotherms of SiSBA-15 (*a*), La_{75}SBA-15 (*b*), La_{50}SBA-15 (*c*), and La_{25}SBA-15 (*d*)

It also is shown in Table 3 that the wall thickness of LaSBA-15 samples is higher than that of SiSBA-15. This observation is in agreement with the TG results and with a recent work [8], and also indicates that a fraction of the initial amount of lanthanum was incorporated within the mesopores in the form of a metallic oxide thin layer, which can also explain the shorter volume and microporous area of LaSBA-15 samples in comparison to the SiSBA-15. This layer within the mesopores may have blocked the micropores, causing the reduction in the volume and microporous area. Moreover, the presence of this layer explains the greater surface area of LaSBA-15 samples in comparison to the SiSBA-15, as it may have caused the increase of wrinkles within the mesopores, causing the increase in the surface area of the LaSBA-15 samples.

Similarly to the TG results, most textural properties has not showed a linear variation in relate to La-content, which can indicate there is a competition between the effects caused by the two forms as the lanthanum was incorporated.

Ethanol dehydration

Figure 4 presents the conversion of ethanol over each sample in relation to reaction time. The catalytic activity of LaSBA-15 samples has been higher than that of SiSBA-15, indicating that the lanthanum incorporation method employed has been efficient to promote active sites in this molecular sieve. One can also observe that the conversion decreases slowly in all tests. This fact indicates a low rate of coke formation, which can be related to the non-formation of high compounds and the high average pore size of the samples, which facilitates the reagents and products diffusion. The non-formation of C4 and of high compounds indicates that samples have not strong acid sites enough to

Table 3 Textural properties of the samples

Sample	S_{BET} (m^2/g)	S_{micro} (m^2/g)	V_p (cm^3/g)	V_{micro} (cm^3/g)	D_p[a] (nm)	a_0 (nm)	w[b] (nm)
SiSBA-15	589.8	90.9	1.46	0.04	7.21	11.33	4.12
La_{75}SBA-15	775.4	73.6	1.31	0.03	4.27	11.86	7.59
La_{50}SBA-15	720.2	54.3	1.18	0.02	5.35	12.14	6.79
La_{25}SBA-15	557.5	72.8	1.49	0.03	5.37	12.44	7.07

[a] BJH pore size calculated from the adsorption branch

[b] $w = a_0 - D_p$

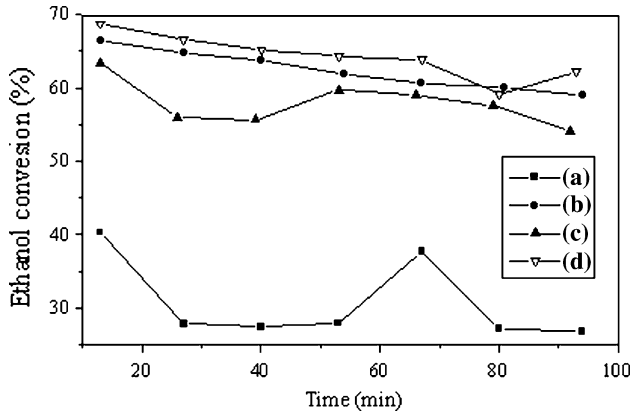

Fig. 4 Ethanol conversion over SiSBA-15 (*a*), La_{75}SBA-15 (*b*), La_{50}SBA-15 (*c*), and La_{25}SBA-15 (*d*) in relation to reaction time

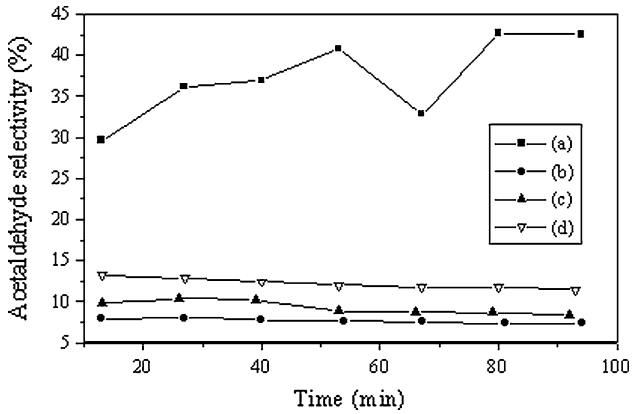

Fig. 6 Acetaldehyde selectivity over SiSBA-15 (*a*), La_{75}SBA-15 (*b*), La_{50}SBA-15 (*c*), and La_{25}SBA-15 (*d*) in relation to reaction time

catalyze olefins polymerization reactions. On the other hand, the samples were able to convert ethanol into water, ethylene, acetaldehyde, and diethyl ether. All the samples have showed low selectivity (<2.5%) to this last product, indicating that the reactions conditions were not favorable to intermolecular dehydration, maybe due to high temperature, as this reaction is exothermic [24]. The ethylene and acetaldehyde selectivity over SiSBA-15 and LaSBA-15 samples is shown in Figs. 5 and 6, respectively. It was observed that ethylene selectivity over LaSBA-15 samples was higher than that over SiSBA-15, and has shifted toward to higher values with the decrease of the La-content. Considering that the ethanol conversion into ethylene by catalytic dehydration is a well-known test reaction for estimating Lewis acidity, these observations indicate that acidity of the SBA-15 increased with the La-incorporation. It also indicates that the acidity of LaSBA-15 samples increases with the decrease of the La-content, which is consistent with the thermal analysis results and textural properties, and reinforces the idea that there has been the formation of a lanthanum oxide thin layer within the mesopores of the LaSBA-15 samples and that the lanthanum fraction incorporated this form increases with the decreasing of the La-content. Other observation that demonstrates the presence of the lanthanum oxide layer in the LaSBA-15 samples is the acetaldehyde formation, whose selectivity has increased with the reducing of the La-content, as shown in Fig. 6. This product is derived from ethanol dehydrogenation, which is catalyzed by a basic site [25]. According to Guan et al. [26], in this case, the ethylene and acetaldehyde formation is an evidence of the presence of metallic oxide in the molecular sieve and that the LaSBA-15 samples have weak Lewis acid and basic functionalities. The lanthanum atom acts like Lewis acid site while the oxygen atom, next to the metal, acts like the basic site.

Also it is observed in Fig. 6 that the SiSBA-15 has showed high selectivity to acetaldehyde. This behavior is attributed to ethanol dehydrogenation over Si–O–Si groups [26], which are present in great quantities in this sample, as suggested by thermal analysis results.

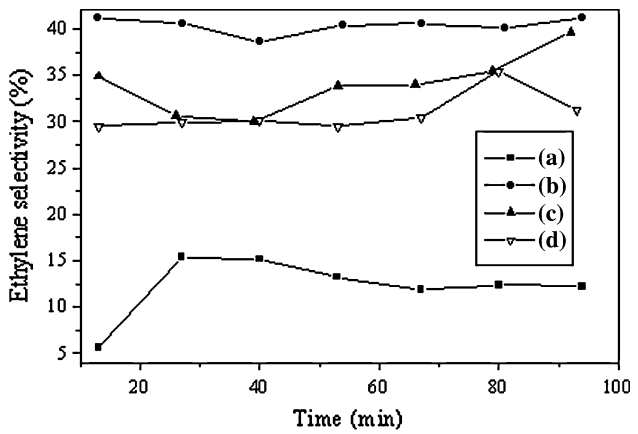

Fig. 5 Ethylene selectivity over SiSBA-15 (*a*), La_{75}SBA-15 (*b*), La_{50}SBA-15 (*c*), and La_{25}SBA-15 (*d*) in relation to reaction time

Conclusion

The characterization of the samples has indicated that the lanthanum was incorporated in two forms in the SBA-15: into the framework and within the mesopores, like a thin layer of lanthanum oxide. These two forms affect competitively the textural properties of the samples impregnated with lanthanum, especially the average pore size. The ethanol dehydration has showed that the LaSBA-15 samples have weak Lewis acid and basic functionalities, indicating the presence of lanthanum oxide in these samples, which has allowed the good conversion of ethanol into water, ethylene, ether and acetaldehyde, with greatest selectivity to ethylene.

Acknowledgements The authors would like to thank the FAPEPI and UESPI for the award of scholarship, the support from the PETROBRAS, ANP, FINEP, and CNPq, and the Institutional X-ray Diffraction Laboratory—UFRN.

References

1. Zhao D, Feng J, Huo Q, Melosh N, Fredrickson GH, Chmelka BF, Stucky GD (1998) Science 279:548
2. Zhao D, Huo Q, Feng J, Chmelka BF, Stucky GD (1998) J Am Chem Soc 120:6024
3. Timofeeva MN, Jhung SH, Hwang YK, Kim DK, Panchenko VN, Melgunov MS, Chesalov YuA, Chang JS (2007) Appl Catal C 317:1
4. Baca M, Rochefoucauld E, Ambroise E, Krafft J, Hajjar R, Man PP, Carrier X, Blanchard J (2008) Micropor Mesopor Mater 110:232
5. Kumaran GM, Garg S, Soni K, Kumar M, Gupta JK, Sharma LD, Rao KSR, Dhar GM (2008) Micropor Mesopor Mater 114:103
6. Gu C, Chia PA, Zhao XS (2004) Appl Surf Sci 237:387
7. Jang M, Park JK, Shin EW (2004) Micropor Mesopor Mater 75:159
8. Mu Z, Li JJ, Hao ZP, Qiao SZ (2008) Micropor Mesopor Mater 113:72
9. Zhang Y, Gao F, Wan H, Wu C, Kong Y, Wu X, Zhao B, Dong L, Chen Y (2008) Micropor Mesopor Mater 113:393
10. Zhou Y, Bao R, Yue B, Gu M, Pei S, He H (2007) J Mol Catal A Chem 270:50
11. Laha SC, Mukherjee P, Sainkar SR, Kumar R (2002) J Catal 207:213
12. Araújo AS, Jaroniec M (1999) J Colloid Interface Sci 218:462
13. Dai Q, Wang X, Chen G, Zheng Y, Lu G (2007) Micropor Mesopor Mater 100:268
14. Shah P, Ramaswamy AV, Lazar K, Ramaswamy V (2007) Micropor Mesopor Mater 100:210
15. Kumar GS, Palanichamy M, Hartmann M, Murugesan V (2008) Micropor Mesopor Mater 112:53
16. Lou Z, Wang R, Sun H, Chen Y, Yang Y (2008) Micropor Mesopor Mater 110:347
17. Selvaraj M, Kawi S (2008) Catal Today 131:82
18. Li Y, Feng Z, Lian Y, Sun K, Zhang L, Jia G, Yang Q, Li C (2005) Micropor Mesopor Mater 84:41
19. Aguado J, Calleja G, Carrero A, Moreno J (2008) Chem Eng J 137:443
20. Szegedi A, Popova M, Minchev C (2009) J Mater Sci 44:6710. doi:10.1007/s10853-009-3600-y
21. Coutinho ACSLS, Quintella SA, Araujo AS, Barros JM, Pedrosa AMG, Fernandes VJ Jr, Souza MJB (2007) J Therm Anal Calorim 87:457
22. Sonwane CG, Ludovice PJ (2005) J Mol Catal A Chem 238:135
23. Chareonpanich M, Nanta-ngern A, Limtrakul J (2007) Mater Lett 61:5153
24. Chen G, Li S, Jiao F, Yuan Q (2007) Catal Today 125:111
25. Chimentão R, Herrera JE, Kwak JH, Medina F, Wang Y, Peden CHF (2007) Appl Catal A Gen 332:263
26. Guan Y, Li Y, van Santen RA, Hensen EJM, Li C (2007) Catal Lett 117:18